

New Approach for the Evolution and Expansion of Space Debris Scenario

M. R. Ananthasayanam*

Indian Institute of Science, Bangalore, Karnataka 560 012, India

and

A. K. Anilkumar† and P. V. Subba Rao‡

Indian Space Research Organization, Trivandrum, Kerala 695 022, India

DOI: 10.2514/1.19623

The evolution of the space debris scenario consisting of a very large number of fragments is described using the propagation of the characteristics of equivalent fragments without propagating each and every individual debris fragment. This is similar to characterizing a fluid in terms of the average density, pressure, and temperature without considering the velocities of individual molecules in a fluid element. The space debris fragments are assigned to a three-dimensional bin of semimajor axis, eccentricity, and ballistic coefficient. A suitably defined representative semimajor axis, eccentricity, and an equivalent ballistic coefficient (a , e , B) are defined for the equivalent fragments in each of the bins. A constant gain Kalman filtering technique based on 1) propagating the above characteristics, and 2) updating them as and when further measurements become available, has been proposed. Further the assimilation of the information from other breakups with the passage of time is also possible. The robustness of the constant Kalman gain approach instead of using the Kalman filter statistics helps to handle better the unmodeled or unmodelable errors due to the finite bin size and the environmental perturbations. This methodology is also suggested to handle massive atmospheric data assimilation problems.

Nomenclature

A	=	reference projected area
a	=	semimajor axis
B	=	($=C_D A/m$, Ballistic coefficient)
C_D	=	drag coefficient
e	=	eccentricity
K_B	=	constant Kalman gain for ballistic coefficient update
K_N	=	constant Kalman gain for number density update
m	=	mass
N	=	number density
P_0	=	covariance matrix of the initial state vector
Q	=	covariance matrix of the state noise
R	=	covariance matrix of the measurement noise
\mathfrak{R}	=	covariance matrix of the innovation
Δ	=	small change in semimajor axis or eccentricity per orbit
v_k	=	innovation

I. Introduction

SOME of the most difficult issues in the study of the evolving low earth orbit (LEO) debris scenario [1,2] are 1) the unpredictable on orbit breakups occurring at random location, intensity and directionality, generating debris clouds made up of enormous number of fragments, 2) the presently existing debris fragments running into thousands for large objects and millions for the smaller ones, 3) the uncertainty of the fragment's physical characteristics such as the mass, shape, and size, 4) the uncertainty of the other important characteristic like the ballistic coefficient (=the product of the drag coefficient and the reference projected area divided by the mass) accounting for the aerodynamic force on

the various fragments and thus change its orbital characteristics, 5) the variability of the perturbations due to air density, gravitational anomalies, lunar solar perturbations, and solar radiation pressure, 6) the debris clouds taking about a few years to merge with the background debris scenario, 7) the uncertainty in the various measurements by radar, optical telescopes, and retrieved satellites and space objects, and 8) any simulated laboratory experiment provides only a sample characteristic of the breakup.

This paper describes a probabilistic estimation theoretic methodology [3] for tracking a group of evolving space debris fragments of various sizes in the LEO and also estimate the so-called equivalent ballistic coefficient for such group of fragments. Some of the compulsive reasons to follow the above methodology are the uncertainty, variability, complexity, enormity of the states and measurements, and the possibility of even deterministic problems be modeled as probabilistic and mathematically treated in suitable ways [3].

For studying the long-term evolution of the space debris, a model [1,2,4] has to be assumed. These models are generally derived by simulating the various historical breakups, assuming some growth rate due to later breakups, and also using the measured data. The long-term predictions of the scenario depend on the qualitative structure and the quantitative parameters in the above model. At large times the prediction could depart greatly from the real scenario due to the sensitivity of the evolution to the inaccuracies in the model or the parameters. As is well known, there are large differences in the estimated number density between many debris models [1,2,5]. The only way the prediction can be made to follow more closely the real situation is to update the predicted value of the states and the parameters by assimilating properly the available measurements at later times. Such updated states and parameters can be used for further evolution in time and later updated using subsequent measurements as and when they become available. Another way of interpreting this is to say that for proper progress "theory" and "experiments" should go together.

The present approach differs from the earlier studies by providing a systematic way of assimilating the information in the measurement data at later times with the present debris scenario. Apart from such "fusion" it also helps to expand the scenario to provide an estimate of the so-called equivalent ballistic coefficient (EQB) of the equivalent

Received 22 August 2005; revision received 26 April 2006; accepted for publication 1 May 2006. Copyright © 2006 by Dr. A. K. Anilkumar. Published by the American Institute of Aeronautics and Astronautics, Inc., with permission. Copies of this paper may be made for personal or internal use, on condition that the copier pay the \$10.00 per-copy fee to the Copyright Clearance Center, Inc., 222 Rosewood Drive, Danvers, MA 01923; include the code \$10.00 in correspondence with the CCC.

*Professor, Department of Aerospace Engineering.

†Scientist, Vikram Sarabhai Space Centre.

fragments (EQF) of the conglomeration of the debris as will be described later. This is just the right kind of situation for utilizing the Kalman filter approach [6] with uncertain or unmodelable terms in the state and measurement equations as well as unknown noise statistics [7,8]. The Kalman filter is able to follow the time evolution of the orbital characteristics such as the semimajor axis “ a ” and the eccentricity “ e ” of the EQF and also derive the EQB [2,8].

The “fusion” of the state and measurement and the parameter updates can be achieved by properly tuning the various statistics in the Kalman filter [6,9]. However, this is well known to be the hardest task in filter design. In this paper first [2–4,8,10] the basic concepts of describing the space debris scenario using the EQF is described followed by the Kalman filter and its implementation, in particular, using the constant Kalman gain approach instead of tuning the filter statistics is presented. The present approach is validated by intensive simulation studies.

II. Present Model for Describing the Evolution of the Space Debris Scenario

A. Concept of Binning

Consider, for example, a satellite moving in space under the influence of various perturbing forces. When the orbital parameters are estimated accurately it is possible to track it. However, after about a week its orbital characteristics are once again estimated based on the measurements to enable continued tracking. If such is the situation for a satellite, one can imagine the amount of task involved in tracking each and every one of the orbital debris fragments. Hence the binning of the fragments based on their near similar orbital and other characteristics is introduced as described below.

The concept of binning of the orbital debris can be understood as follows. Consider the molecules in a small fluid volume though which the molecules move in and out. The gross macroscopic properties such as density, mean velocity, or temperature are the ones in which one may be interested instead of the individual microscopic mass and velocity of each of the molecules in the fluid volume. Thus a compression of information is taking place. Similarly, when we consider the debris in fixed semimajor axis and eccentricity bins, we are handling a suitably defined average property. However, we do not have that many fragments in small volume as in fluid flows which exhibit asymptotically certain transport characteristics that can be theoretically derived. For the debris fragments the error due to coarseness of the (a, e) bin size does remain and in order to characterize their properties and limit the error one needs periodic update through measurements. A more detailed comparison of the differences between the orbital space debris and gas molecules is provided in Table 1.

B. Characteristics of the Equivalent Fragment in Terms of the Fragments in a Bin

A simplification as mentioned in the previous section is to bin the debris fragments in discrete intervals of semimajor axis, eccentricity, and ballistic coefficient. Presently we have used a total of $(10 \times 10 \times 10)$ bins, with 10 divisions for each of the parameters a , e , and B formed by splitting their expected range. Another important simplification that makes the problem tractable is that the various slices of the “ B ” bins can be considered to be independent though the ballistic coefficient of the EQF can meander across the bins. This is somewhat similar to a single object with a constant value of the ballistic coefficient moving in the atmosphere. In general, it is possible for the space objects to change their orientation in the orbit, or the gas-surface interaction to alter the drag coefficient and hence the ballistic coefficient.

Then instead of handling every fragment, the conglomeration of all the fragments in every bin is handled as an EQF. Then it is necessary to assign suitable values for the EQF properties in terms of the individual fragment properties to help follow the dynamics of the conglomeration of EQF. This poses a conceptual problem. A priori how well a mathematically defined quantity can help to follow the dynamics is not clear. Even the mean can be arithmetic, geometric, or harmonic or any other. Further, the numerical value of such a quantity is later updated in the filter. Can the updated values be equal to the defined quantity at all subsequent times? In general, it cannot be true. At best we can use the initially defined and subsequently updated value to track the conglomeration in some acceptable way. Based on all the individual fragments in a bin, we initially assign for the EQF the arithmetic mean for its semimajor axis and the geometric mean for the eccentricity and the ballistic coefficient.

C. Evolution of the Individual Fragments and the EQF in the Bins

The state variables are initialized to the scenario at initial time. At present a large number of about 10,000 simulated debris fragments due to an explosion are considered and later the additional fragments due to further breakups are accounted for as source terms. The state propagation equations for both the fragments and the EQF are similar. The rate of change over one revolution in the elements “ a ” and “ e ” due to drag alone for the k th revolution is given by

$$a_k = a_{k-1} + \Delta a_{k-1} \quad e_k = e_{k-1} + \Delta e_{k-1}$$

where a_k , e_k stand for semimajor axis and eccentricity, respectively, at time instant k with the change per revolution denoted by Δ being functions of the density at the perigee height, density scale height, rotation of the atmosphere, mass, drag coefficient, and effective reference area following King-Hele [11,12].

The EQF is propagated based on its assigned value of suitable a and e and could in general end up in just within another bin.

Table 1 Differences between orbital space debris and gas molecules^a

No.	Feature	Gas molecules	Orbital space debris
1	History	Studied for centuries	Studied for about a few decades
2	Flow regimes	Free molecular to Continuum	Free molecular
3	Constituents	Equal size, shape and mass	Unequal size, shape and mass
4	Evolution	Binary collision among themselves and any body in space	Mainly convection and at times collision
5	Environment	Similar molecules and body	Randomly varying atmosphere, Earth's gravitational harmonics, Solar Radiation Pressure, Luni Solar Perturbations.
6	Distribution function	$f(r, v, t)$	$f(r, v, m, S, t)$
7	Source terms	Generally not present	Source due to explosions and collisions and sink terms due to decay are present
8	Periodic measurements	Not essential (theory is adequate)	Essential
9	End objective	Forces and heat transfer experienced by the body.	Risk analysis, orbit selection among many other uses
10	Present status of subject	Well developed theory with experimental supplement	Not fully developed. Difficult for theory and experiment

^a r = location in space; v = velocity; m = mass; S = cross sectional area; t = time.

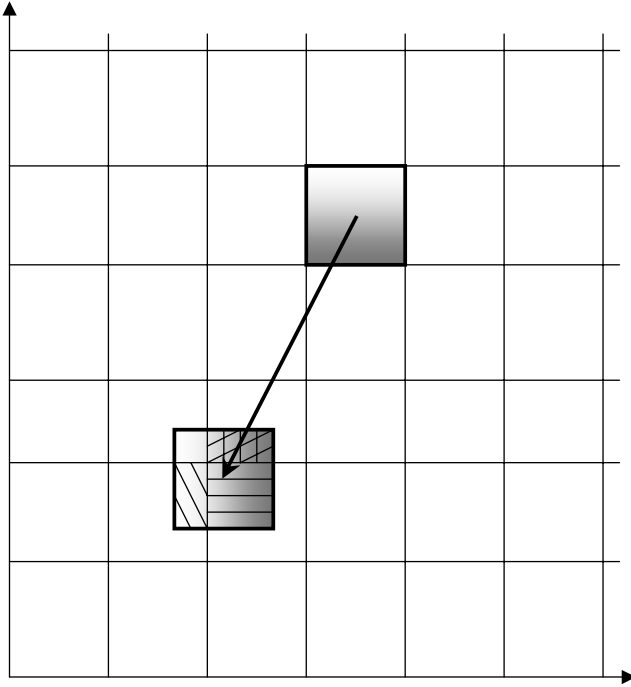


Fig. 1 Graphical representation of the orbital propagation algorithm in the eccentricity e vs semimajor axis a space.

However, the various fragments of which the above is made could end up in the surrounding bins as well. To mimic such a feature a proposed heuristic rule is to redistribute the fraction of the EQF among the bins. Such a rule as in Rossi et al. [4,13,14] takes the ratio between the area covered by the propagated rectangle and the area of the rectangle itself as shown in Fig. 1. Later due to the launches and retrievals the changed debris number density, their orbital parameters, and the ballistic coefficient are also accounted.

Later, by using the measurements the EQB of each EQF is updated based on the weighted average of the predicted and measured number density of the fragments in the bins. This weightage is the Kalman gain, as we will see later on. It will be shown subsequently if there is no update of this EQB of these EQF, then there is a drift with time of the predicted number density from the true values, and when there is an update, the filter is able to follow closely the true time variation of the number density of the debris fragments in the various bins. This is the reason to call the ballistic coefficient of the EQF as the equivalent ballistic coefficient (EQB).

D. Update of the EQF Characteristics

The present model carries out the evolution of the EQF in two steps, namely

- 1) The propagation of the EQFs representing all the fragments in the various bins. The next task is to redistribute the fragments with some weightage around the adjacent bins based on some simple rule as mentioned above. Further if there are any further breakups these are also accounted for the changed number density in the various bins.

- 2) Provide an improved estimate of the number density of the fragments in the various bins and also update the equivalent ballistic coefficient of the EQFs both by utilizing appropriate constant Kalman gains. The constant gains are obtained by minimizing a suitable cost function by using the genetic algorithm [15,16] as will be explained later.

There is one subtle point in the estimation of the EQB of the EQF corresponding to various (a, e) bins. After update the value of B for the EQB of EQF at times can fall outside the bin interval. Such a thing could be surprising because we mentioned earlier that range of the “ B ” bins are fixed. The equivalent B formed out of individual fragments cannot have the ballistic coefficient outside this range. However there is a subtle approximation that has occurred. Each time

the EQF is propagated, it is from the location based on the arithmetic and geometric mean of the (a, e) bin as mentioned earlier. There is a loss of information with regard to the true (a, e) coordinates of the individual fragments. The propagation of the EQF is always from the above initial condition based on the above means. But for a conglomeration of fragments such an initial condition may not be the most appropriate. The EQF with slightly different mathematically defined properties could have started its trajectory from the corners or the edges or anywhere in the (a, e) bin at which time the redistribution could have been different and so also the updated ballistic coefficient B .

E. Comparison of the Present Approach with the Stochastic Analog Tool of Rossi et al.

The first step in the present procedure is somewhat similar to the treatment in the stochastic analog tool (STAT) of Rossi et al. [13]. The STAT code simulates the time evolution of the debris environment by considering the number of objects contained in a set of discrete bins of semimajor axis, eccentricity, and mass. The evolution algorithm is based upon a set of finite difference equations, which take into account launches, retrievals, explosions, collisions, and orbital propagation under the influence of atmospheric drag. In STAT the bins are provided by a threefold subdivision, namely 1) in the semimajor axis from 6378 to 46378 km, 2) eccentricity from 0 to 1, and 3) mass from 1 mg to 10,000 kg. The state variables are initialized at the actual population, which is taken from the CNUCE 1994.0 orbital debris reference model [14]. Once the variables have been initialized, the calculation and summation of different contributions at each time step are performed.

It may be noted that the present approach considers 1) a , 2) $\log(e)$, and 3) $\log(B)$ for the threefold division as against a , e , and m of STAT. The third parameter B has been presently used because the orbital parameters are sensitive to the air drag and thus change with time. A question that would occur is that in general there could be errors due to discretization and approximation in specifying the mean values for a and e in the various bins and further in the propagation due to unaccounted or even unmodelable forces. Such errors can be accounted for by process noise in the state equations describing the propagation of the EQF. An important feature of the present approach as in STAT is that because the individual representative object of each bin is propagated the computing time is almost independent of the debris population size.

It is the second step that is fundamentally new and different in the present approach. A brief description of the estimation theory leading to the Kalman filtering equations and the present constant Kalman gain approach is provided in Appendix A. For a more rigorous treatment of Kalman filtering one can refer to the book by Maybeck [17]. The relative weightage in terms of the Kalman gains provided by the filter depends on the combination of the statistics of the process and measurement noises [6,7,9,18]. In general, after the initial transients the Kalman Gain matrix tends to a constant value in many such problems like rendezvous and docking [18], and reentry of space objects [10] when state modeling errors are present. Further, instead of tuning the noise statistics it is efficient to tune the various Kalman gains in the filter [2,10]. Hence the present constant Kalman gain approach for treating the evolution of the orbital debris scenario and the update at a measurement. In the second update step apart from assimilating the measurement information it also expands the scenario to update the EQB for the EQFs.

III. Real-World and Filter World Scenarios

The state and measurement equations in the real world and filter world scenarios are given in Tables 2 and 3, respectively, to provide an appreciation of the present approach using Kalman filtering. It is very interesting to see that in the state equations of the filter world scenario the coarser conditions brought about by the binning, forming the EQF, propagation, and redistribution lead to modeling error and thus need process noise. In the present simulation studies the propagation of each and every one of the individual debris fragments and counting their number in the various bins leads to no

Table 2 Real-world scenario without binning

Quantity	Description
The state variables	(a, e, B) of each of the individual fragments.
The state input	Suitable model for the complex environment.
The state noise	Random variations in real situation from the above model environment.
The initial state	Fragment characteristics based on ASSEMBLE or any other suitable model.
The measured variables	The number of fragments in the various bins.
The measurement noise	Measurement errors in the orbital characteristics assigned to the individual debris fragment due to errors in tracking and data processing.

Table 3 Filter world scenario with binning (in the present simulation studies)

Quantity	Description
The state variables	(a, e, B) of the EQF in each of the bins propagated and redistributed and also accounting for fragments from additional breakups.
The state input	Suitable model for the complex environment. Presently only the air drag effect is considered.
The state noise	The unmodelable inaccuracies in assigning the values for (a, e, B) for the EQF and its further propagation, redistribution, and also the environment.
The initial state	Fragment characteristics based on ASSEMBLE or any other suitable model to obtain the EQF.
The measured variables	The (a, e, B) for each of the individual fragments as in the real world but propagated with atmospheric drag alone and later converted to the number of objects in each of the bins.
The measurement noise	In the present simulation there is no measurement noise because all the fragments are propagated and based on the changed values of the orbital parameters (a, e) they are assigned to the appropriate bins.

measurement noise. In a real-world scenario, there would be measurement noise due to inaccuracies in the assigned orbital characteristics of the individual fragments.

Under these conditions it is useful to invert the role of the above state and measurement equations. Thus, we are able to reach a situation as in the output error method (OEM) where the state equations have no noise but the measurement equations have noise. In the inverted roles of the state and measurement equations the measurement noise arises from binning, forming EQF, propagation, and redistribution as mentioned earlier.

The next question to be answered is how in the present study using the Kalman filter the steady-state constant Kalman gains (implying process noise) have been derived when there is no process noise. It is now useful to understand the purpose in introducing the process noise in Kalman filtering. There are two main uses, namely

1) Modeling: Whenever there are modeling inaccuracies one can inject the process noise to either account, offset, or even estimate quantitatively the above modeling deficiency.

2) Learning: Estimation of the unknown parameters in the deterministic or the probabilistic models in the state or measurement equations.

The first involves stochastic modeling by using the white Gaussian noise or even higher order Gauss Markoff process as is appropriate in the state or measurement equations. Thus, a stochastic process is able to handle a deterministically unmodelable situation. The second involves learning by using the measurements. The present work uses mainly the second feature.

In the present problem there are uncertainties in the initial EQB values attached to the EQF in the state equations in Table 3 (but presently in the measurement equation). The Kalman filter approach improves the estimate of the EQB values of the EQF. Thus using a certain length of data the filter helps to update the suitable values of the EQB for the EQF at various measurement times. Obviously the accuracy of estimation depends on data length.

Now it is clear why the process noise is introduced implicitly into the filter through the estimation of the constant Kalman gains. Based on a simple exercise of estimating a constant signal without process noise but corrupted with measurement noise as in Ananthasayanam et al. [3,8] different constant Kalman gains affect the duration of the transient and the steady-state error. A smaller process noise leads to longer transient but lower steady-state error, and vice versa. In the present study, based on a certain length of data used for deriving (or equivalently minimization of an appropriate cost function) the constant Kalman gains have been derived, as will be explained in the next section.

IV. Constant Gain Kalman Filter Approach

Assuming the number of debris fragments in each three-dimensional (a, e, B) bins are known from simulation exactly, it is explained as to how the Kalman filter by using the updated number of objects and the constant gains is able to track closely the true number of fragments. This section also explains how the measurements can be assimilated and the scenario expanded to obtain the equivalent ballistic coefficient.

A. Filter World State Equations

Here, attention can be given to various EQF, which are specified by these parameters:

- 1) The number of fragments in the particular (a, e) bin,
- 2) The equivalent semimajor axis,
- 3) The equivalent eccentricity, and
- 4) The equivalent ballistic coefficient.

The first parameter is clear and the second is arithmetic, with the third and fourth being the geometric mean of the fragments in the bins. The (a, e) bins are not changing and the EQF moves in the (a, e) plane like any other single fragment and later gets redistributed based on a certain rule. Thus the states presently considered in each and

every one of the (a, e) bins are the number of objects N and their equivalent ballistic coefficient B .

The measurements are just the number of fragments in the above (a, e) bins. The state equations for the EQF in the various bins between measurements are

$$\begin{aligned} dN/dt &= \Sigma[\text{propagation across the } (a, e) \text{ bins} + \text{redistribution} \\ &\quad + \text{source terms}] + \text{state noise} \\ dB/dt &= 0 + \text{state noise}(=0) \end{aligned}$$

B. Filter World Measurement Update Equations

The measured quantities are only the true number density N_M in the various bins. These are obtained in simulation by propagating each and every one of the individual debris fragments. It is this that is used to update the predicted number density from the EQF propagation and redistribution to an improved value and also update the ballistic coefficient of the EQF in the various bins based on equations such as

$$N^+ = N^- + K_N(N_M - N^-) \quad B^+ = B^- + K_B(N_M - N^-)$$

with the superscript $(+)$ and $(-)$ denoting, respectively, the post- and preupdated values. The constant Kalman gains K_N and K_B correspond, respectively, to the number density and the equivalent ballistic coefficient. In the constant Kalman gain approach the number of such gains to be estimated is 200 namely the two K_N and K_B for each of the (a, e) bins. These can be obtained by minimizing the cost function

$$J = \sum \mathbf{v}_k^T [\mathfrak{R}]^{-1} \mathbf{v}_k$$

where the innovation $\mathbf{v}_k = (N_M - N^-) = (\text{measurement value} - \text{model prediction})$, and \mathfrak{R} is the covariance matrix of the innovation. The \sum denotes the summation over all bins and times. If one uses \mathbf{P}_0 , \mathbf{Q} , and \mathbf{R} (see Appendix A) there could be some variation in the gain values during the transient and the steady-state conditions. Assuming the \mathfrak{R} to be constant it can be estimated similar to the estimation of \mathbf{R} in the method of maximum likelihood estimation with measurement noise alone or better known as output error method (OEM). Thus, a set of constant Kalman gains can also be worked out based on the above cost function J by utilizing a proper optimization algorithm.

Such constant Kalman gains have been obtained by using the genetic algorithm [15,16] as briefly explained in Appendix B. In the GA each member of the population will thus have 200 values of gains. The different parameters used in the GA implementation after some trial and error are also provided in Appendix B. The Kalman gains obtained by following the 10,000 objects was also used subsequently without any change, to follow the evolution with more breakup and source terms.

The major part of the simulation time is taken up to follow the orbital characteristics of each and every one of the 10,000 individual fragments. Later the 100 EQFs have to be propagated in each slice of B to form the cost function. Obviously this has to be repeated over the population size and generations. It takes about 100 h of computer time in a MATLAB environment (though not CPU) using a 1.7 MHz PC to obtain the results of each of the test cases discussed here. Though such a computing time is not presently uncommon, the present interest is to derive the constant gains by following one single breakup alone and subsequently using the same gains to demonstrate the adequacy to follow the evolution with more breakups, and source terms. Such an approach shows the way in which a certain model of the space debris scenario can be followed for longer times.

V. Case Studies and the Analysis of the Results

First, we consider the evolution of the debris clouds generated due to one single explosion. Later, we add more breakups and further source terms at arbitrary times during the evolution.

A. Evolution of Debris Objects Generated due to Explosions

To study the effect and the soundness of the above approach, a single explosion is simulated using the ASSEMBLE model [2,19,20]. Considering an explosion, at a typical altitude of 800 km and eccentricity 0.00045, about 10,000 objects of varying ballistic coefficients were simulated. These objects were propagated by taking into account only the atmospheric drag effect for a period of 600 days and thus the basic measurement data of the number of objects in the three-dimensional (a, e, B) bins is generated.

B. Evolution of a Single Breakup

Three different approaches are possible to follow the number density of the fragments with time. These are

Case A: updating number of objects alone,

Case B: updating only the EQB, and

Case C: updating both the number density and the EQB.

In all of the subsequent figures the symbol \circ denotes the measurements (in this case the state) and representing the true values of the number density of the fragments in the bin. The state (in this case the measurement) contains process noise. The filtering process can reduce the effect of the error on the estimates, but not below a certain value due to continuous occurrence of error due to binning, propagation, and redistribution. The dashed line represents the results without any update, meaning the Kalman gain is zero and thus at all times the update equals the prediction. The solid line shows the present results from the Kalman filter with nonzero Kalman gain.

C. Case A: Updating Only the Number Density Alone

The first cases led to most of the constant gains being close to unity of around 0.95 and the results slowly diverge away from the true values. Hence without the estimation of the important parameter

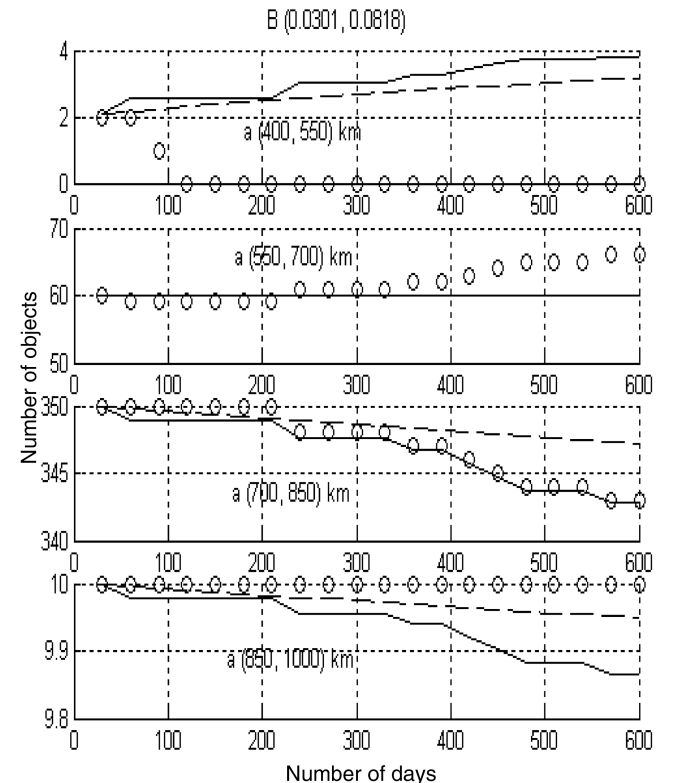


Fig. 2 Updating the ballistic coefficients only using constant gains for B bin (0.0301, 0.0818) (\circ) true; (solid line) filter; (dashed line) no update.

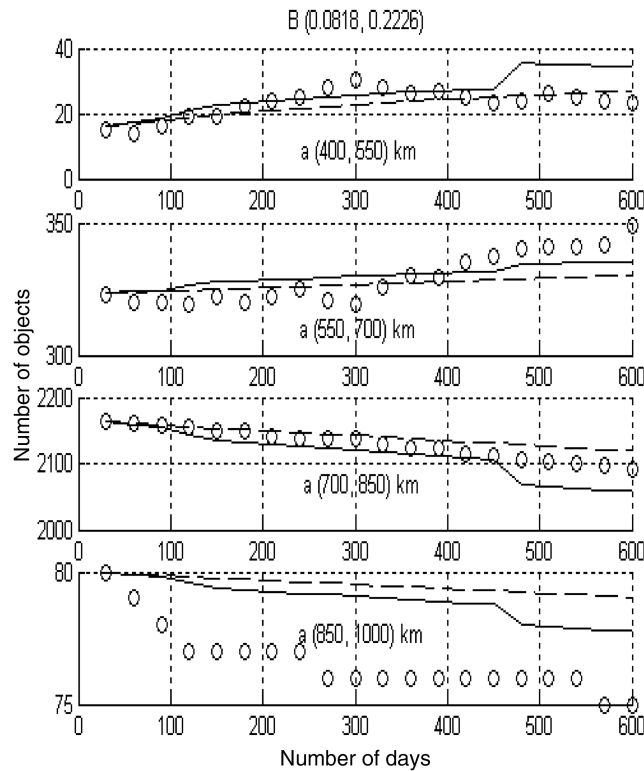


Fig. 3 Updating the ballistic coefficients only using constant gains for B bin (0.0818, 0.2226) (○) true; (solid line) filter; (dashed line) no update.

namely the equivalent ballistic coefficient the results do not have much value.

D. Case B: Estimating the Number of Objects by Updating the EQB Alone

Those bins having a small number of fragments behave numerically not quite properly and the bins with very small values of B are not sensitive to drag and, thus, hardly change their orbital parameters. Hence hence it is not easy to update their values. Only the intermediate bins with a fair number of fragments and responding to the drag are amenable for appropriate updates of the B are discussed in the following sections. Thus, the present results are mostly discussed across the 1) semimajor axis bins between the kilometer intervals (400,550), (550,700), (700,850), and (850,1000), which generally possess a reasonably large number of fragments.

Figure 2 provides the results for the above case by updating B alone for the lower B bin (0.0301, 0.0818). Even though the number densities of the fragments are not updated, in those cases in which there are many fragments (as between 700 and 850 km) the filter estimates are close to the measurements. Also one can note that there is a definite improvement in the estimation for the number of objects over the one without filter update. Figure 3 corresponding to the medium B bin (0.0818, 0.2226) shows the estimates are better with filtering than without filtering and in particular with more fragments. Figure 4 for the higher B bin (0.6056, 1.6476) shows a similar behavior as in the previous cases.

E. Case C: Estimating the Number of Objects by Updating both the Number Density and the EQB

Figures 5 and 6 show the results for the third case where the filter updates have been provided for both the number density and the EQB and filter results are even better than the previous two cases and closer to the true values. Figure 5 provides the results for the above case for the lower B bin (0.0301, 0.0818). It may be noted that at all perigee altitudes the filtered estimates are closer to the true number of objects shown by the ○ symbol. Figure 6 for the higher B bin (0.6056, 1.6476) shows a very good tracking behavior of the filter as for the earlier two bins. Thus one can summarize that the best results

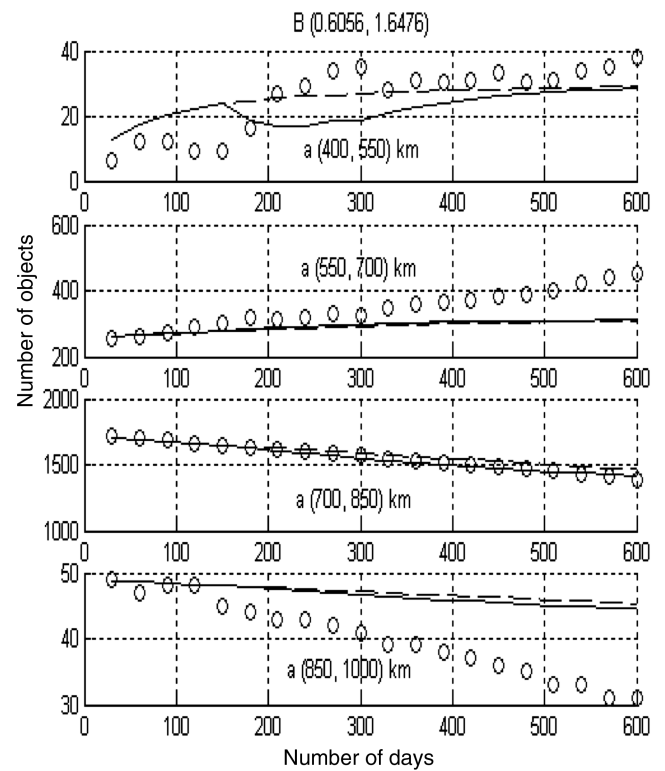


Fig. 4 Updating the ballistic coefficients only using constant gains for B bin (0.6056, 1.6476) (○) true; (solid line) filter; (dashed line) no update.

are obtained when the number density and the equivalent ballistic coefficients are both updated.

F. Variation of the Constant Kalman Gain for the Number of Fragments in Case C

Figure 7 shows the variation for the constant Kalman gain across the semimajor axes bins for four ballistic bins. It may be noted that the Kalman gains for the number density are always between zero and unity. This happens, obviously, because the state namely the number density is also a measured quantity. The gains show some variations across the semimajor axes.

However one may hope and see that some constancy appears to exist for the gains across the a bins. Next assuming a single constant gain of 0.5 for the number density across all the a bins the GA was run. It turned out that the filter updates were able to track the number of objects quite as well as in the previous Case C of Figs. 5 and 6 which had varying gains across the a for the number density. The gains in this simpler case turned out to be between 0.4 and 0.6 for various ballistic coefficient ranges.

In Kalman filter generally the gains are more robust variables than the values of the statistics of the initial state, process noise, and measurement noise covariance values. The different combinations of the above noise statistics can lead to the same gain. Further even the constant Kalman gain appears to be robust in its own right in the following way. When the filter was run with modest changes in the constant gains generally one notices that there is not much of a change in the results. Such a behavior has been reported by Phillip [18] in the rendezvous and docking problem. The advantage of such a result is that far fewer numbers need to be stored to run the Kalman filter and in particular for on line real time applications.

In contrast the behavior of the constant gains for the ballistic coefficient shown in Fig. 8 can be positive or negative for various values of the semimajor axes bins. This can happen because the ballistic coefficient though a state has not been measured. Second it may be noted that a single value for the constant gain is not suitable to obtain the update of the ballistic coefficient across all the semimajor axes. Such a formal constant value led to unsatisfactory results. Figure 9 shows variation of the estimated ballistic coefficient with

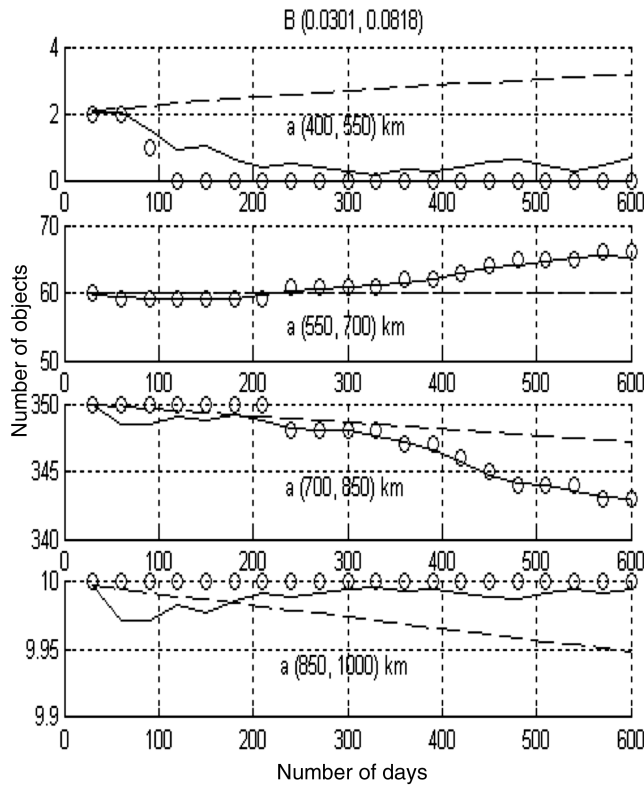


Fig. 5 Updating the ballistic coefficients and number of objects using constant gains for B bin (0.0301, 0.0818) (○) true; (solid line) filter; (dashed line) no update.

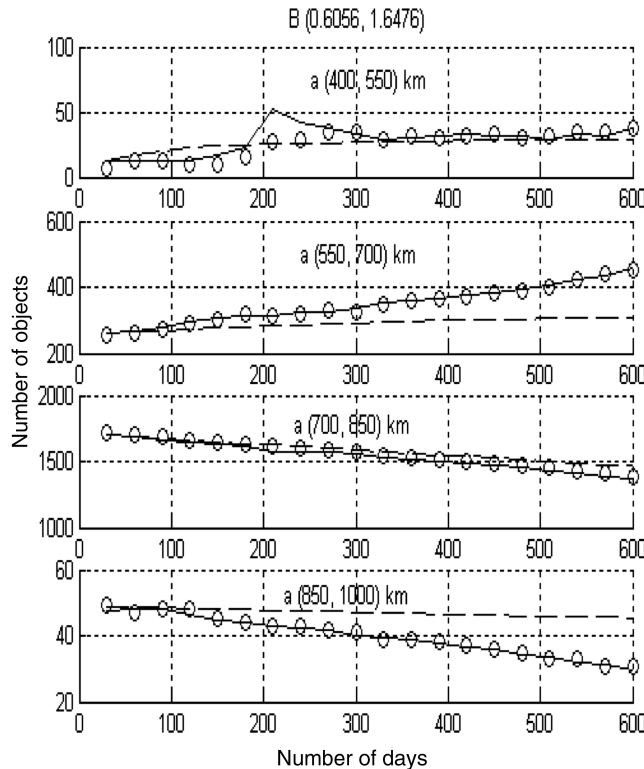


Fig. 6 Updating the ballistic coefficients and number of objects using constant gains for B bin (0.6056, 1.6476) (○) true; (solid line) filter; (dashed line) no update.

time in four typical bins. It may be noted that the estimates are generally within the limits of the ballistic coefficient bins. However, at times they move somewhat outside the limits of the bin values. At present, the initial condition for EQF propagation is always from the

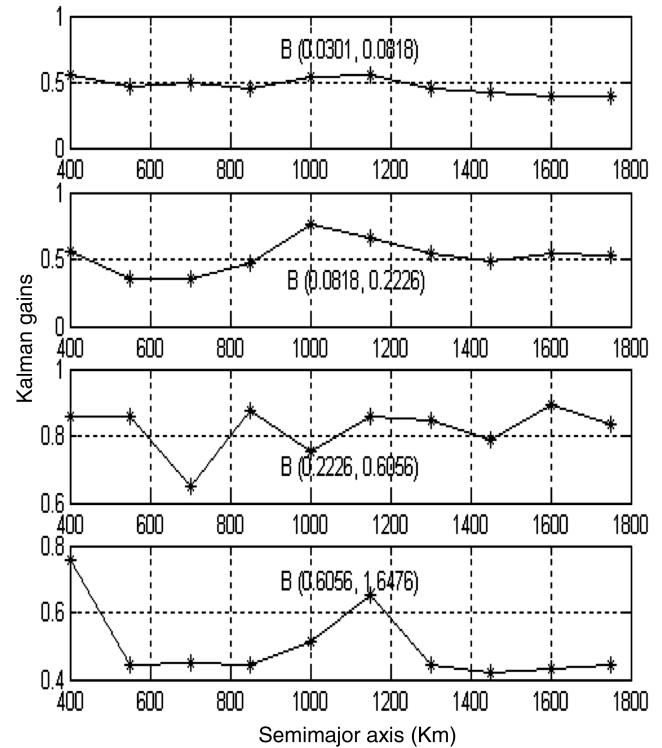


Fig. 7 Kalman gains for number of objects (K_N).

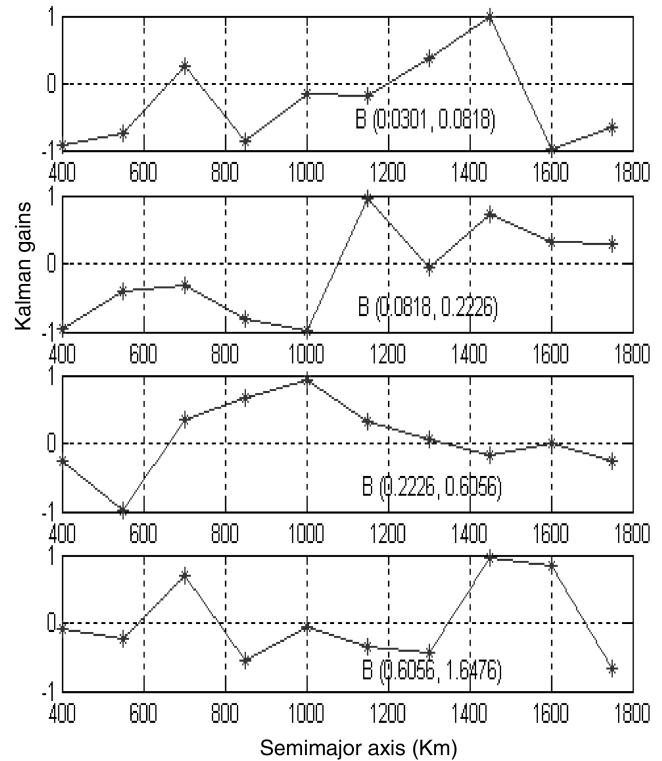


Fig. 8 Kalman gains for ballistic coefficients (K_B).

mean values of the bins, although it could have started from anywhere, including the corners or the sides. The subsequent propagation and redistribution error due to such initial conditions of the individual fragments could be responsible for such a behavior. It is hence best to think of the various means defined here as a formal mathematical specification with some acceptable mathematical ability to mimic the dynamical behavior.

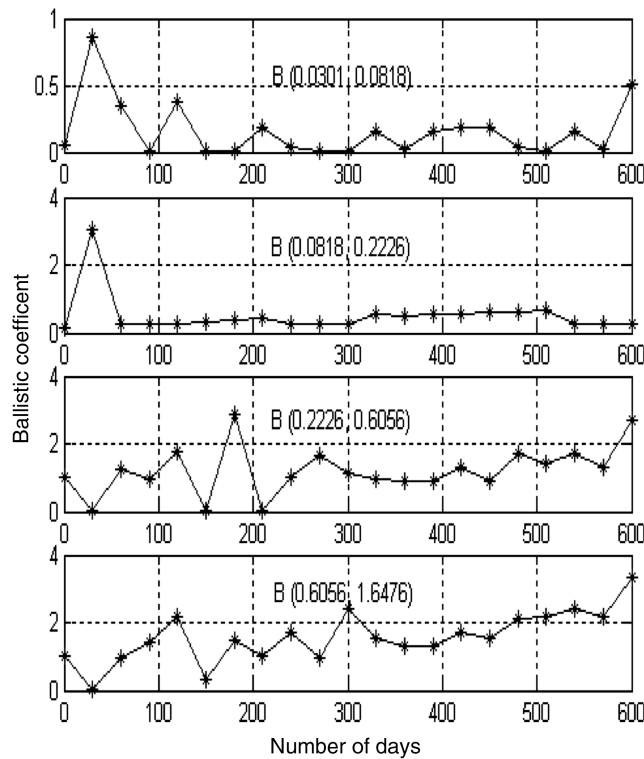


Fig. 9 The estimated ballistic coefficients.

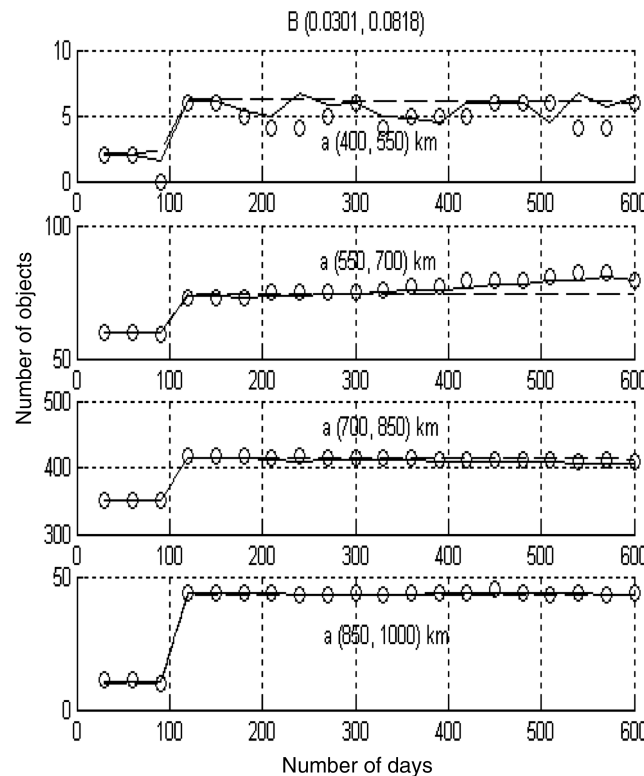


Fig. 10 One source of explosion included. Updating the ballistic coefficients and number of objects using constant gains for B bin (0.0301, 0.0818) (○) true; (solid line) filter; (dashed line) no update.

G. Case C: Evolution of a Single Breakup Followed by Another Breakup

This forms the further test case for the results and in particular the various constant Kalman gains derived from the previous case C of an evolving breakup followed for 600 days. The values of the constant gains have been used even in the present scenario, namely

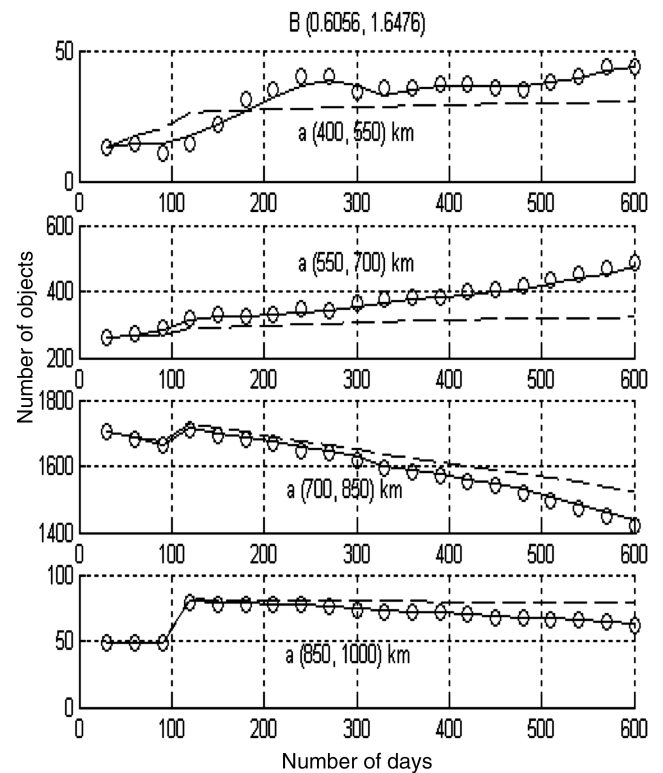


Fig. 11 One source of explosion included. Updating the ballistic coefficients and number of objects using constant gains for B bin (0.6056, 1.6476) (○) true; (solid line) filter; (dashed line) no update.

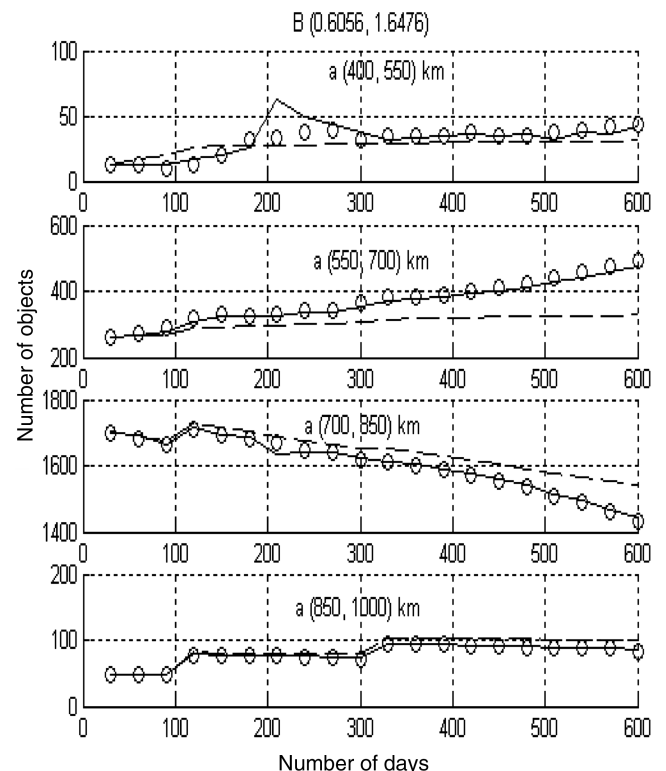


Fig. 12 Comparison between estimated and observed number of objects: two sources of explosions included. Updating the ballistic coefficients and number of objects using constant gains for B bin (0.6056, 1.6476) (○) true; (solid line) filter; (dashed line) no update.

after the first breakup at the beginning, the second breakup was introduced after 120 days. One might be tempted to wonder if all the results including the constant Kalman gains should be reworked. It turns out to be unnecessary to rework the results for the constant gains. The derived values from the earlier case C are able to follow the present evolution involving two breakups and are demonstrated in the latter sections. Slower changes in the dynamical behavior can be tracked by using the earlier values of the gains. After 10,000 fragments were introduced at the beginning and additionally 300 fragments were introduced after 120 days. Such a situation is similar to what is happening in the real-world scenario of debris creation. The debris is growing but not at too rapid a rate when compared with the existing population.

The constant Kalman gains obtained based on the debris cloud evolution have been used even after adding the source terms. The robustness of the constant gains, in other words the performance of the filter around a range of the estimated gains, is the reason behind the above behavior, even if the results are nonoptimal, they will be adequate to obtain acceptable estimates. The behavior of the filter is shown in Figs. 10 and 11 for the two ballistic coefficient bins, namely lower and higher, respectively. Note that the filter tracks the number density variation in all the ballistic coefficient bins very well and in particular after the introduction of the new breakup.

H. Case C: Evolution of a Single Breakup Followed by More than One Breakup

Further, the concept of utilizing the constant gains obtained for a single breakup for tracking slowly varying further breakups is demonstrated with the introduction of two breakups at different time steps, one at 120 days and another at 330 days. Figure 12 for a typical higher bin shows the behavior of the filter and it can be described as quite good. It can be noticed that the filter without any update is generally unable to follow the true number density values.

I. Case C: Evolution of a Single Breakup Followed by More than One Breakup and Some Launch Activities

Further, to simulate the real-world scenario of space debris sources, some launch activities such as, say, satellites and rocket bodies are introduced during the evolution of the breakup clouds. Here we added at random times a maximum of 5 objects (0 to 5) together with the latter two breakup sources. It may be noted that once again the constant gains obtained using the primary debris clouds alone are the ones that are continued to be used in all the later cases as well. The results of this study are provided in the Fig. 13. This figure shows that the present model is able to track the number of objects in the evolution process and also update the ballistic coefficient B . The behavior of the filter even in such cases is quite good.

VI. Analysis of a Typical Real-World Scenario

We now demonstrate the application and use of the above approach in a typical real-world scenario. We consider the debris objects in near circular orbits in the perigee and apogee bin of 700 to 800 km catalogued in the TLE data for 1 yr from October 1998 to September 1999. The TLE sets for the 335 objects used were el981016.txt, el981110.txt, el981209.txt, el990109.txt, el990211.txt, el990311.txt, el990409.txt, el990513.txt, el990611.txt, el990710.txt, el990808.txt and el990912.txt obtained from the TLE achieves. Figure 14 provides the distribution of the objects in the semimajor axis bins initially from the first TLE set.

This situation in a small 100-km range is very helpful and computationally efficient for applications involving collision probability analysis with the passage of time. An initial ballistic coefficient is assumed for the equivalent fragments that is propagated and updated using first eight observations, and the next three estimators are with the estimated B at the eighth month. This analysis also shows it to be possible to make further certain simplifications like constant eccentricity for all the equivalent fragments in all the bins because the bin size is just 10 km unlike in the simulated

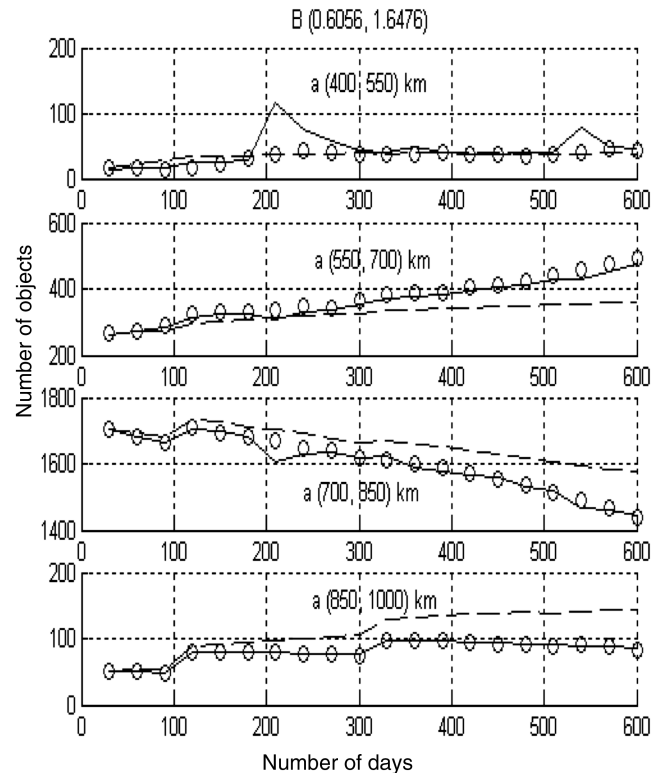


Fig. 13 Comparison between estimated and observed number of objects: two sources of explosions and some new launches included. Updating the ballistic coefficients and number of objects using constant gains for B bin (0.6056, 1.6476) (○) true; (solid line) filter; (dashed line) no update.

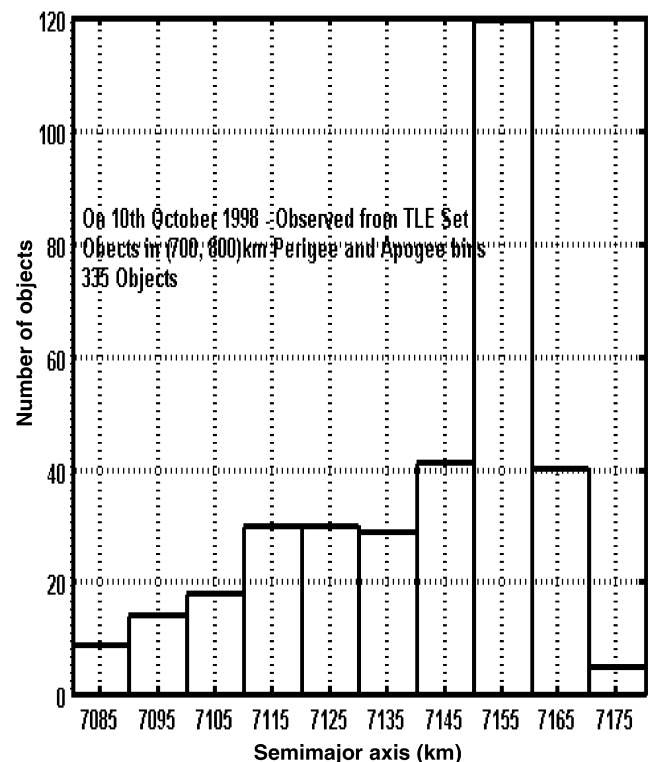


Fig. 14 Initial distribution of the debris number density with semimajor axis.

scenario where it was 150 km but their semimajor axis corresponds to the mid value of the bin. The Kalman gains that were used were obtained from simulation studies. This demonstrates the robustness of the constant Kalman gains. The innovation here is given by the

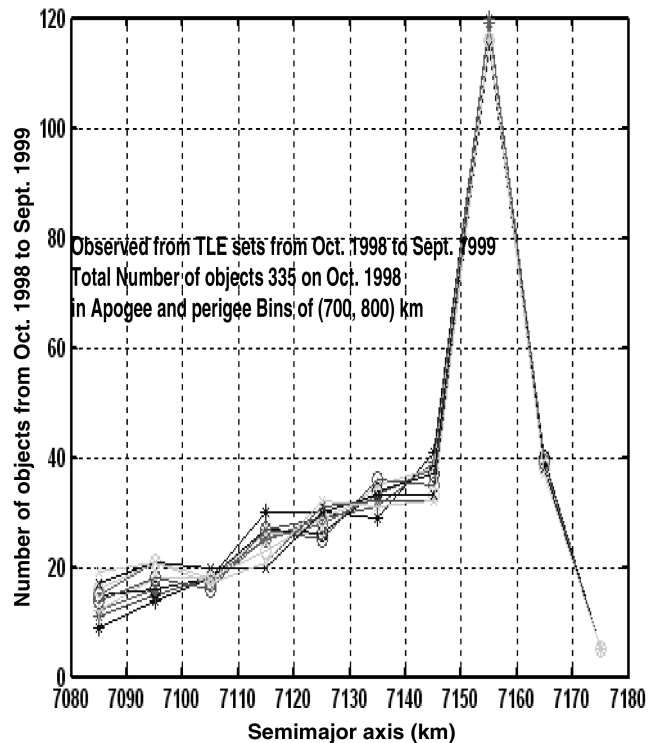


Fig. 15 Variation of the number density of the debris in the bins with time.

difference between the TLE data and the predicted number density. However, it is to be noted that should the gains be taken as zero, thus, no update, then the filter cannot track the debris or much less update the important ballistic coefficients, and the filter estimates will diverge with increasing time from the TLE data values.

The 335 objects observed in the apogee/perigee bin for October 1998 were tracked for the next 12 months to obtain the

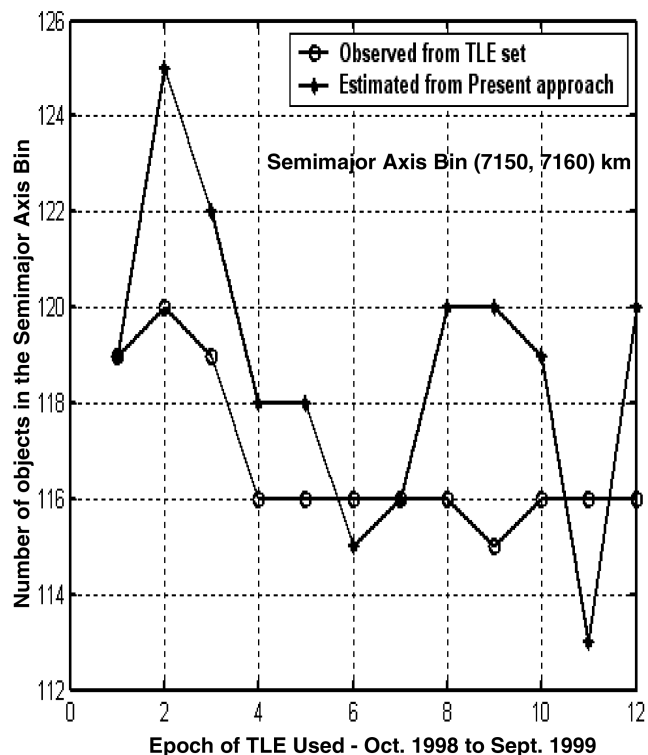


Fig. 16 Comparison of the estimated time varying debris number density with TLE values in the bin (7150, 7160) km during a year.

number of objects in the semimajor axis bins. The orbital elements were propagated up to a single TLE epoch of 17th of the month 00.00 h in the analysis. Figure 15 provides the number of objects for the 12 months in different semimajor axis bins by tracking the same objects.

Figure 16 provides a comparison of the number of objects obtained from the present approach with that of the observed for the semimajor axis bin of (7150, 7160) km. It may be seen that the number of objects matches quite well even by propagating 10 equivalent objects rather than propagating and monitoring all of the 335 objects.

To summarize, this approach, using constant Kalman gain, is recommended by us to handle massive real-world atmospheric data assimilation problems [21] that are presently studied using the filter statistics that are far more difficult to tune as is the propagation of the state covariance equations demanding massive amounts of computer time.

VII. Inference of the Distribution of the Fragment Properties from the EQF Characteristics

At this stage one might think whether it would not be possible to infer the distribution of the individual fragment characteristics from the EQF. In forming the EQF there is some loss of information. Hence, if the inverse problem has to be solved, it would involve introducing an additional information, innovation, or assumptions into the EQF characteristics. Perhaps if there are some well known asymptotic properties as for a gas in thermodynamic equilibrium at a given temperature one can then say that the distribution of the individual velocities follows a Maxwellian distribution (as the physicists call the same Gaussian distribution) of the kinetic theory of gases. But no such results are presently available in the present situation for orbital debris. Also we have seen earlier that some of the characteristics of the debris obey certain distributions such as normal, lognormal, or Laplace and so on. Generally with just one single parameter it is not possible to make a guess regarding the probability distribution.

If instead of using the constant Kalman gain approach the more involved approach of working with the statistics of the initial state, process, and measurement noise covariances in the Kalman filter we could have arrived at another parameter characterizing the dispersion of the characteristic parameters. Here we have the subtle feature of the Kalman filter describing the result in terms of the normal distribution with the estimate and the covariance for linear systems. For nonlinear systems the normal distribution approximates the behavior of the estimates. Even then the computational burden of handling the present problem in terms of estimating the above statistics is far more than by the constant gain route. Such a route would appear to defeat the very purpose of simplicity of the present constant gain Kalman filter approach. The present approach is just about the simplest providing the best possible results.

VIII. Conclusions

A novel innovative approach based on the propagation of an equivalent object in a three-dimensional bin of semimajor axis, eccentricity, and the ballistic coefficient (a, e, B), together with a constant gain Kalman filter technique, is described in this paper. This new approach propagates the number density in a bin of a and e rapidly without propagating each of the individual debris fragments in the above bins. Further, this approach expands the scenario to provide suitable ballistic coefficient values for the EQFs in the various bins. It is able to assimilate the measurement information with the passage of time from other breakups as well. The heart of the technique is to use a constant Kalman gain, which is nearly optimal and able to track the dynamically evolving fragment scenario and further expand the scenario to provide appropriate time varying EQB for the EQF in the various bins. The present approach of constant gain Kalman filter involving thousands of debris fragments can be fruitfully used even in massive atmospheric data assimilation problems that have tens of thousands of states and measurements.

Appendix A

I. Brief Outline of Estimation Theory and Constant Gain Kalman Filter Approach

In estimation theory a nonlinear continuous system with time “ t ” with discrete measurements is described by

$$\begin{aligned} d\mathbf{X}/dt &= \mathbf{F}(\mathbf{X}, \mathbf{U}, \boldsymbol{\Theta}, t) + \mathbf{w}(t); & \mathbf{X}(0) &= \mathbf{X}_0 \\ \mathbf{Z} &= \mathbf{G}(\mathbf{X}, \mathbf{U}, \boldsymbol{\Theta}, t_k) + \mathbf{v}(t_k); & \mathbf{k} &= 1, 2, \dots, N \end{aligned}$$

where \mathbf{X} , \mathbf{Z} , $\boldsymbol{\Theta}$, \mathbf{U} , \mathbf{w} , and \mathbf{v} denote, respectively, the states, measurements, unknown parameters, control inputs, state and measurement noise matrices. The process and measurement noise are assumed to be white with zero mean and covariance \mathbf{Q} and \mathbf{R} , respectively. The time evolution of the estimate and covariance of the state \mathbf{X} in terms of the transition matrices ϕ and ψ from local linearization and the measurements are

$$\begin{aligned} \mathbf{X}_k^- &= \phi_{k-1} \mathbf{X}_{k-1} + \psi_{k-1} \mathbf{U}_{k-1}; & \mathbf{X}(0) &= \mathbf{X}_0 \\ \mathbf{P}_k^- &= \phi_{k-1} \mathbf{P}_{k-1} \phi_{k-1}^T + \mathbf{Q}_k; & \mathbf{P}(0) &= \mathbf{P}_0 \\ \mathbf{Z}_k &= \mathbf{H}_k \mathbf{x}_k + \mathbf{v}_k \end{aligned}$$

The $(-)$ denotes the estimate before using the measurement information. Thus at time t_k an estimate \mathbf{X}_k^- with covariance \mathbf{P}_k^- and the measurement namely \mathbf{Z}_k with covariance \mathbf{R}_k can be combined statistically to obtain

$$\begin{aligned} \mathbf{X}_k^+ &= \mathbf{X}_k^- + \mathbf{K}_k [\mathbf{Z}_k - \mathbf{H}_k \mathbf{X}_k^-] = \mathbf{X}_k^- + \mathbf{K}_k \mathbf{v}_k \\ \mathbf{P}_k^+ &= [\mathbf{I} - \mathbf{K}_k \mathbf{H}_k] \mathbf{P}_k^- [\mathbf{I} - \mathbf{K}_k \mathbf{H}_k]^T + \mathbf{K}_k \mathbf{R}_k \mathbf{K}_k^T \end{aligned}$$

where \mathbf{v}_k called as the innovation. For minimum \mathbf{P}_k^+ the optimal Kalman gain is given by

$$\mathbf{K}_k = \mathbf{P}_k^- \mathbf{H}_k^T [\mathbf{H}_k \mathbf{P}_k^- \mathbf{H}_k^T + \mathbf{R}_k]^{-1}$$

The innovation follows a Gaussian distribution whose probability when maximized leads to the method of maximum likelihood estimation (MMLE), which operationally is to minimize the cost function

$$\begin{aligned} \mathbf{J} &= (1/N) \sum \mathbf{v}_k [\mathbf{H}_k \mathbf{P}_k^- \mathbf{H}_k^T + \mathbf{R}_k]^{-1} \mathbf{v}_k^T = (1/N) \sum \mathbf{v}_k^T [\mathfrak{H}] \mathbf{v}_k \\ &= \mathbf{J}(\mathbf{X}_0, \mathbf{P}_0, \mathbf{Q}, \mathbf{R}, \boldsymbol{\Theta}) \end{aligned}$$

based on summation over all the number of measurements denoted here by N . When $Q \equiv 0$, MMLE is called as output error method (OEM) all the Kalman gains are zero. In various applications the Kalman Filter needs compulsively the “a priori” statistics \mathbf{P}_0 , \mathbf{Q} , and \mathbf{R} , which may not be known and difficult to estimate. Usually in many problems after the initial transients the Kalman gain matrix tends to a constant value due to inaccurate system, input, and/or the measurement model. In such cases the constant Kalman gains can also be worked out to minimize the above J by utilizing an optimization algorithm assuming \mathfrak{H} to be constant. The advantage of the above is one need not propagate the covariance equations resulting in enormous decrease in the computations.

Appendix B

Genetic algorithm (GA) has recently emerged as a very robust stochastic optimization method by mimicking nature and Darwin’s theory of survival of the fittest. It turns out to be efficient due to features like the coding of the parameter set and not the parameter themselves, uses cost but not the gradients of the cost function, and uses probabilistic and not deterministic transition rules. In a simple genetic algorithm an initial generation of individuals are randomly chosen in the search space. The next generation is created after applying three operators in their order of execution such as 1) *reproduction*: individuals are copied to the next generation with probability relative to their fitness, 2) *crossover*: pairs of strings drawn randomly from the population are subjected to crossover.

They are randomly paired to create two new descendants. For each pair a crossover location in the bit string is selected at random, which divides the string into two parts. Swapping the remainder of the two strings with each other does crossover, and 3) *mutation*: after mutation a bit is randomly selected within the chromosome string and mutated. The termination criteria could be after a fixed number of generations, or the change in fitness value between populations. The various steps adopted for the implementation of GA are given below.

1) Choose a coding to represent problem parameters and the criteria for reproduction, crossover and mutation, as well as the initial population size, probabilities of cross over and mutation, search domain of the variables, and a termination criteria.

2) Set $T = 0$, and generate an initial population from the search domains randomly.

3) Evaluate each string of the population for fitness. If termination criteria is satisfied then STOP.

4) Perform reproduction, crossover, and mutation on the population and evaluate the strings of the new population.

The parameters used in the present GA implementation after some trial and error are the population size = 200; bit length = 20; probability of crossover = 0.90; probability of mutation = 0.05; Convergence: number of generations = 50 or alternately change in J between generations = 0.0001.

Acknowledgments

A. K. Anilkumar would like to acknowledge the support provided by Vikram Sarabhai Space Centre, Indian Space Research Organisation, in pursuing his research on space debris at the Indian Institute of Science, Bangalore, India. Also he would like to thank the Department of Aerospace Engineering, Indian Institute of Science, for extending necessary facilities in pursuing the research. The authors would like to thank the referee for his valuable comments that helped to improve the paper to a greater extent.

References

- [1] Johnson, N. L., and McKnight, D. S., *Artificial Space Debris*, Orbit Book Company, Malabar, FL, 1991.
- [2] Anilkumar, A. K., “New Perspectives for Analyzing the Breakup, Environment, Evolution, Collision Risk and Reentry of Space Debris Objects,” Ph.D. Thesis, Department of Aerospace Engineering, Indian Institute of Science, India, 2004.
- [3] Ananthasayanam, M. R., Anilkumar, A. K., and Subba Rao, P. V., “Evolution of the Orbital Debris Scenario based on Kalman Filter Approach,” Indian Institute of Science, Fluid Mechanics Rept. 2004 FM 2, Department of Aerospace Engineering, Bangalore, February 2004.
- [4] Rossi, A., Cordelli, A., Farinella, P., Anselmo, L., and Pardini, C., “Long Term Evolution of the Space Debris Population,” *Advances in Space Research*, Vol. 19, No. 2, 1997, 331–340.
- [5] Anon., “Technical Report on Space Debris”; text of the report adopted by the Scientific and Technical Subcommittee of the United Nations Committee on the Peaceful Uses of Outer Space, United Nations, New York, 1999.
- [6] Kalman, R. E., and Bucy, R. S., “New Results in Linear Filtering and Prediction Theory,” *Journal of Basic Engineering*, Vol. 83D, 1961, pp. 95–108.
- [7] Ananthasayanam, M. R., “Fascinating Perspectives of State and Parameter Estimation Techniques,” AIAA Paper 2000-4319, 2000.
- [8] Ananthasayanam, M. R., Anilkumar, A. K., and Subba Rao, P. V., “Evolution and Expansion of the Orbital Debris Scenario Based on Constant Gain Kalman Filter Approach,” Report IAC-04-IAA5.12.1.10, 2004.
- [9] Ananthasayanam, M. R., “A Relook at the Concepts and Competence of the Kalman Filter,” AIAA Paper 2004-571, 2004.
- [10] Anilkumar, A. K., Ananthasayanam, M. R., and Subba Rao, P. V., “Prediction of Re-Entry of Space Debris Objects: Constant Gain Kalman Filter Approach,” AIAA Paper 2003-5393, August 2003.
- [11] King-Hele, D., *Satellite Orbits in an Atmosphere: Theory and Applications*, Blackie, Glasgow and London, 1987.
- [12] Vallado, D. A., *Fundamentals of Astrodynamics and Applications*, 2nd ed., Kluwer Academic, Norwell, MA, 2001.

- [13] Rossi, A., Cordelli, A., Farinella, P., and Anselmo, L., "Collisional Evolution of the Earth's Orbital Debris Cloud," *Journal of Geophysical Research*, Vol. 99, No. E11, 1994, 23,195–23,210.
- [14] Rossi, A., Anselmo, L., Cordelli, A., Farinella, P., and Pardini C., "Modelling the Evolution of the Space Debris Population," *Planetary and Space Science*, Vol. 46, Nos. 11,12, 1998, pp. 1583–1596.
- [15] Whitley, L. D., *Foundations of Genetic Algorithms*, Morgan Kauffmann Publishers, San Francisco, CA, 1993.
- [16] Deb, K., *Optimization for Engineering Design: Algorithms and Examples*, Prentice-Hall, New Delhi, India, 1995.
- [17] Maybeck, P. S., *Stochastic Models, Estimation, and Control*, Vol 1, Academic Press, Inc., New York, 1979; Vol. 2, Academic Press, Inc., New York, 1982.
- [18] Philip, N. K., "A Study of the Estimation Schemes with Controller for the Final Phase of a Rendezvous and Docking Mission of Spacecraft," Ph.D. Thesis, Department of Aerospace Engineering, Indian Institute of Science, Bangalore, July 2001.
- [19] Anilkumar, A. K., Ananthasayanam, M. R., and Subba Rao, P. V., "A Posterior Semistochastic Low Earth Debris On-Orbit Breakup Simulation Model," *Acta Astronautica*, Vol. 57, November 2005, pp. 733–746.
- [20] Anilkumar, A. K., Ananthasayanam, M. R., and Subba Rao, P. V., "Simulation of Some Historical On-Orbit Breakups Using ASSEMBLE Model," AIAA Paper 2003-5760, January 2003.
- [21] Bouttier, F., and Courtier, P., *Data Assimilation Concepts and Methods*, "Training Course Notes of European Centre for Medium Range Weather Forecasts," Reading, U.K., 1999.

I. Boyd
Associate Editor